Scanning Microscopy

Volume 2 | Number 1 Article 19

9-24-1987

The Surface Characterization of Modified Chrysotile Asbestos

J. K. De Waele
University of Antwerp

F. C. Adams
University of Antwerp

Scanning Microscopy, Vol. 2, No. 1, 1988 (Pages 209-228) 0891-7035/88$3.00+.00
Scanning Microscopy International, Chicago (AMF O'Hare), IL 60666 USA

THE SURFACE CHARACTERIZATION OF MODIFIED CHRYSOTILE ASBESTOS

J.K. De Waele and F.C. Adams*

Department of Chemistry, University of Antwerp (U.I.A.)
Universiteitsplein 1, B-2610 Wilrijk, Belgium

(Received for publication March 06, 1987, and in revised form September 24, 1987)

Abstract

In this paper, results of a semi-quantitative and qualitative leaching study of chrysotile and Chrysophosphate® fibers in oxalic acid and succinate salt buffer solutions with laser microprobe mass analysis (LAMMA) and electron probe X-ray micro-analysis (EPXMA) are presented, which demonstrate clearly the potential of these sensitive surface analytical tools for the analysis of natural, physico-chemically modified and depleted fibers. These results are verified with those obtained by atomic absorption spectroscopy (AAS) for the measurement of the leached magnesium and iron concentration in solution. In order to study differences in adsorption behaviour and reaction capability between natural and chemically modified chrysotile, LAMMA-analysis was performed on fibers treated with benzo[a]pyrene, N,N-dimethylaniline (DMA) and ortho-phenylene-diamine (OPDA). In correlation with biomedical investigations, this study could contribute to the elucidation of the potential sequences of fiber surface properties in relation to the biological activity and cytotoxicity.

KEY WORDS : Laser microprobe mass analysis (LAMMA), surface characterization, chrysotile asbestos fibers, Chrysophosphate® fibers.

*Address for correspondence :
F. Adams, Department of Chemistry, University of Antwerp - U.I.A., Universiteitsplein 1, B-2610 Wilrijk (Belgium). Phone No. (03)828.25.28.

Introduction

Of particular interest to both producers and users of asbestos fibers is the potential health problem allegedly associated with asbestos exposure (Becklake, 1983 ; McDonald, 1985 ; Doll and Peto, 1985). Because of the apparent pathogenicity of asbestos, there has been a general reaction of the public and certain health authorities regarding the use of products containing the material. This had led to research to modify asbestos fibers in such a way as to reduce as much as possible the undesirable biological effects (Ménard et al., 1986 ; Lalancette and Dunnigan, 1981 ; Kimmerle et al., 1982 ; Dunnigan et al., 1980).

There are several reports dealing with the modifications of certain physico-chemical properties to improve filtration characteristics, enhanced tensile strength, improvement of flame resistance, water-proofing for the manufacture of water repellent fabrics, dispersion of the fibers, and reduction of the emission during handling and use of finished asbestos-containing products (Cook and Smith, 1979 ; Derricott, 1979).

Various materials have been proposed which interact with the surface of asbestos fibers in order to reduce its haemolytic activity. Such materials include disodium ethylenediamine tetraacetic acid (EDTA), simple phosphates, polyvinylpyridine N-oxide and aluminium (Macnab and Harington, 1967), and certain acidic polymers (Schnitzer and Pundsack, 1970). Some of these materials, such as EDTA, are solubilized in body fluids and cannot reduce permanently the long term haemolytic activity of asbestos. Therefore, there is a need to determine materials which will remain adhered to the asbestos fibers. Such passivating materials should not adversely affect the useful commercial properties of asbestos. It has also been found that asbestos fibers treated with metal molybdate (Pezzoli, 1979a) or metal tungstate (Pezzoli, 1979b) have a reduced haemolytic activity in comparison with untreated asbestos fibers.

Recently, a method has been reported for treating chrysotile asbestos fibers by depositing phosphate groups on the fiber surface through a

gaseous $POCl_3$ treatment (Mènard et al., 1986 ; Société Nationale de l'Amiante, 1981). The thus treated chrysotile fibers are named Chrysophosphate® and have been found to possess reduced haemolytic activity as evidenced by experiments with red blood cells, and also reduced cytotoxicity using the rat pulmonary macrophage test (Dunnigan et al., 1980). The preliminary research data indicate that the treatment results in modifications of the infrared spectrum, and of thermal analysis and zeta potential characteristics (Mènard et al., 1986 ; Kimmerle et al., 1982). More importantly, they also show a significant modification which relates to the alleged promoter, or co-carcinogenic effect of asbestos fibers : the reduction of the ability to adsorb some known initiators of lung carcinogenesis present in tobacco smoke (Mènard et al., 1986). In a strategy to design safer fibers, the latter observation is of great significance.

In this paper, we report the results of experiments in which untreated and $POCl_3$-treated chrysotile fibers were analyzed using laser microprobe mass analysis (LAMMA) in order to characterize the fiber surface before and after treatment with different inorganic and organic probes and correlations with results obtained with other analytical tools.

Materials and Methods

Samples

The chrysotile asbestos samples used in this study were provided by Canadian Johns Manville Ltd. through the Chrysophosphate® - SNA Inc. (Société Nationale de l'Amiante), and are classified as "Québec Standard Grade QS 4-T-30" with specific area : 13 $m^2.g^{-1}$ (BET) and zeta potential +18 mV (Mènard et al., 1986). These samples contain fibers with a broad distribution of lengths which were specified from dry screening procedures showing ca. 80 % of the fibers between 1 and 4 μm and ca. 40 % near 2 μm (Jolicoeur et al., 1981 ; Chrysotile Asbestos Test Manual, 1974).

Chrysophosphate®, (Lalancette and Dunnigan, 1981) is obtained by passing N_2 gas, saturated with $POCl_3$ vapors at 14°C through a reaction vessel held at ambient temperature. The concentration of phosphorus permanently retained on the Chrysophosphate® fibers is about 2.2 %. The specific surface area is 4 $m^2.g^{-1}$ and zeta potential is -36 mV (Mènard et al., 1986).

Reagents

- benzene, 99+%, spectrophotometric grade, Gold Label, Janssen Chimica, Belgium ;
- hydrogen chloride (0.1 N), Titrisol, Pro Analysi, Merck, FRG ;
- hydrogen peroxide (30 wt. % solution in bidistilled water), A.C.S. Reagent, Janssen Chimica, Belgium ;
- N,N-dimethylaniline (DMA), 99 %, Janssen Chimica, Belgium ;
- ortho-phenylenediamine (OPDA), 99 % Pro Analysi, Merck, FRG ;
- benzo[a]pyrene (BaP), 99+ %, Gold Label, Janssen Chimica, Belgium ;
- oxalic acid, 99 %, Pro Analysi, Merck, FRG;
- succinate salt-buffer (SSB) solution : 18.51 g sodium succinate, 24 g NaCl, 0.6 g KCl and 2.25 g succinic acid is dissolved in 3 l bidistilled water ; about 3 ml of an aqueous 0.1 % (wt/v) solution of phenol red is added to observe visually small changes in pH value. The SSB-solution (pH = 7.4) is used at 37°C (Hronovsky et al., 1975).

Sample preparation

Leaching experiments : About 30 mg of the chrysotile and Chrysophosphate® standard fibers was suspended in 30 ml oxalic acid solutions of different analytical concentration : 0.050 M (pH = 1.50), 0.100 M (pH = 1.28) and 0.666 M (pH = 0.78). Most experiments were performed in a non-stirred medium. Treatment times were between 5 min and 208 h while treatment temperatures ranged from 20 to 80°C. Some standard samples were also treated for long times (between 24 and 888 h) in a succinate salt-buffer solution at 37°C to imitate *in vivo* leaching behaviour.

At the end of each experiment, the samples were filtered on a Schleicher & Schüll filter (no. 589[1] Schwarzband, Ø110 mm), washed twice with 15 ml of bidistilled water, and recovered for the measurement. Aliquots of the filtrate were diluted with water in order to measure the leached amount of Mg and Fe with atomic absorption spectroscopy (AAS). Present detailed work on the leaching of P and Cl will be published later.

Organic adsorption and catalytic oxidation experiments :

Benzo[a]pyrene (BaP) : To a 30 mg chrysotile or Chrysophosphate® sample, 20 ml of a 10^{-3} M BaP solution in benzene was added. The suspension was refluxed at a temperature of 60°C for 15 h. The fibrous samples were filtered over a Schleicher & Schüll filter (no. 589[1] Schwarzband, Ø110 mm) and rinsed twice with a pure benzene solution (De Waele et al., 1983a).

N,N-dimethylaniline (DMA) : A solution of 15 ml of H_2O_2 (6 %), 20 ml of a 5 % DMA solution in benzene and 30 ml of 0.1 N HCl was added to 40 mg chrysotile or Chrysophosphate® fibers at room temperature. The heterogeneous mixture was stirred for 21 h, filtered off and recovered for analysis (De Waele et al., 1983b).

Ortho-phenylenediamine (OPDA) : A 0.1 M aqueous solution of 25 ml OPDA in the presence of 15 ml of 0.1 N HCl, and 15 ml of H_2O_2 (6 %) was added to 40 mg chrysotile or Chrysophosphate® fiber portions. The heterogeneous mixture was stirred for 17 h at room temperature, filtered off, washed with bidistilled water and recovered for analysis (De Waele et al., 1984a).

Instrumentation

The commercially available laser microprobe mass analyzer (LAMMA®-500, Leybold-Heraeus, Cologne, FRG) is described in detail in the literature (Denoyer et al., 1982 ; Vogt et al., 1981 ; Verbueken et al., 1985 ; De Waele and Adams, 1985). The instrument is able to analyze very rapidly and with high sensitivity both organic and inorganic species present in a microscopic region of a sample. The laser energy exciting a single particle can be varied with a

set of attenuating filters over a useful range, providing complete vaporization of a micrometer size sample at high irradiance, and laser desorption (LD) conditions (Tabet and Cotter, 1983 ; Van der Peyl, 1984 ; Fletcher et al., 1984) at low laser irradiance. When LD-conditions are applied to asbestos, the fibers remain visibly intact and the characteristic mass spectrum of the material vanishes to an insignificant intensity with surface impurities becoming apparent as the only significant mass spectral features (De Waele and Adams, 1985, 1986). The asbestos fiber samples are easily mounted for analysis, e.g., by touching Formvar® film coated electron microscope grids to the powder and shaking off nonadhering material.

For electron probe X-ray microanalysis (EPXMA) a JEOL JXA-733 Superprobe equipped with a Tracor Northern Si(Li) energy-dispersive detection system was employed, using 25 keV electron bombardment in the backscattered electron detection mode. More detailed microstructural fiber information was obtained using a JEOL 1200EX electron microscope, at 80 keV electron bombardment.

Concentration measurements of characteristic elements (Mg, Si, O, P, Cl) at the outer surface layers of the standard chrysotile and Chrysophosphate® fibers, were performed using X-ray photo-electron spectroscopy (XPS) with a Hewlett Packard HP-5950 A spectrometer (AlK_α radiation, 1486 eV) equipped with a hemispherical electrostatic analyzer, a resistive anode electron detector and multichannel analyzer.

The bulk chemical composition of pure and some oxalic acid treated fiber samples was measured using energy-dispersive X-ray fluorescence spectroscopy (ED-XRF), equipped with a Siemens Kristalloflex 2H high-voltage generator, an AG W61-T X-ray tube with tungsten anode, and a Kevex-Ray Si(Li)detector.

Magnesium and iron concentration measurements of the leaching filtrate solutions were performed with a Perkin-Elmer 3030 atomic absorption spectrophotometer (AAS) (Perkin-Elmer Corp., Norwalk, CT, USA).

Results

Characterization of standard chrysotile and Chrysophosphate® fibers

Morphology of chrysotile fibers : Among the various asbestos minerals of industrial interest, chrysotile is by far the most important. Its morphology and main structural and chemical features have been established through investigations using a variety of analytical and physical methods, for example, electron microscopy (Chisholm, 1983 ; Yada, 1971), infrared spectroscopy (Gadsden et al., 1970 ; Luys et al., 1982), X-ray diffraction (Whittaker, 1953, 1955, 1956), surface adsorption (Gorski and Stettler, 1974 ; Nauman and Dresher, 1966), and laser microprobe mass analysis (De Waele et al., 1984b).

Chrysotile asbestos belongs to the category of serpentine minerals (with antigorite and lizardite) all with chemical composition $3MgO.2SiO_2.2H_2O$. Its basic structure consists of a sheet of silica tetrahedra which is overlaid with a sheet of magnesium hydroxide (brucite). The latter is joined to the silica layer by two out of three -Mg-O groups as illustrated in Figure 1A. Because of differences in the lattice parameters of the silica and brucite layers, the composite layer adopts a curvature with the Mg-OH groups on the external surface (Jolicoeur et al., 1981). The growth of these curved sheets, in concentric or spiral arrangements, has led to the naturally occurring fibrils which are found in the form of cylinders with internal and external diameters of approximately 10 nm and 25 nm respectively. It has been suggested that the central cavity of these cylinders contains amorphous minerals, the composition of which varies depending on the origin of the chrysotile (Hodgson, 1979 ; Zussman, 1979).

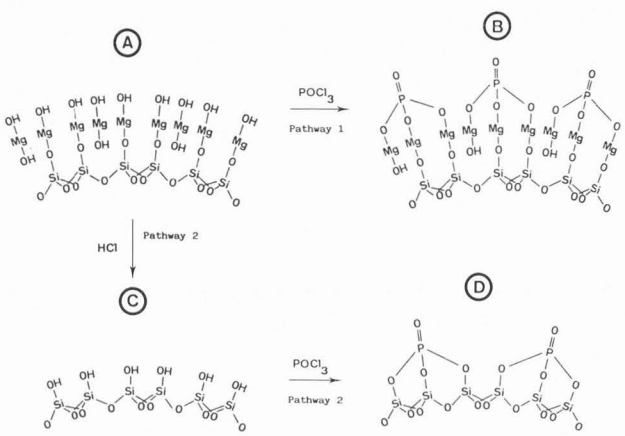

Fig. 1. Cross-sections of a chrysotile fiber showing the composite silica-brucite layer (A) and its reaction with gaseous phosphorus oxytrichloride (B,C,D).

Reaction of chrysotile with phosphorus oxytrichloride

Water adsorbed onto the chrysotile fibers hydrolizes $POCl_3$ to phosphoric acid with production of HCl. According to Lalancette and Dunnigan (1981) and Cossette (1983), the nature of gaseous $POCl_3$ to chrysotile fibers can be described through the reaction paths A to B and A to D via C shown in Figure 1, as cross-sections through the surface of a fiber.

Reaction 1 :

The produced hydrogen chloride reacts with the chrysotile outer surface layers to form silanol groups :

$$[\equiv Si\text{-}O\text{-}Mg\text{-}OH]_3 + 6\ HCl \rightarrow$$

$$[\equiv Si\text{-}OH]_3 + 3\ MgCl_2 + 3\ H_2O \qquad (1)$$

In this reaction $MgCl_2$ and reaction water are formed as by-products.

Reaction 2 :

The formed silanol groups react with the $POCl_3$ to produce an insoluble combination :

$$[\equiv Si\text{-}OH]_3 + POCl_3 \rightarrow$$

$$[\equiv Si\text{-}O\text{-}]_3\ P{=}O + 3\ HCl \qquad (2)$$

The produced hydrogen chloride serves the first reaction.

Reaction 3 :

Meanwhile, gaseous $POCl_3$ reacts directly with the chrysotile outer surface layers to form an insoluble phosphate combination together with hydrogen chloride :

$$[\equiv Si\text{-}O\text{-}Mg\text{-}OH]_3 + POCl_3 \rightarrow [\equiv Si\text{-}O\text{-}Mg\text{-}O\text{-}]_3P{=}O + 3\ HCl \quad (3)$$

Infrared spectroscopy, thermogravimetric analysis X-ray photon spectrometry and X-ray analysis

Ménard et al. (1986) performed infrared spectroscopy and thermogravimetric analysis on the product. The comparison of infrared (IR) spectra of phosphated and non-treated chrysotile fibers indicates an increase in the intensities of OH^- vibrations at 3400 cm^{-1} and 1650 cm^{-1}, and a broadening of the peaks at 1020 cm^{-1} and 1080 cm^{-1}, attributed to the Si-O stretching modes of chrysotile. The increase in the intensities of bands at 3400 cm^{-1} and 1650 cm^{-1} corresponding to free hydroxyl stretching vibrations is attributed to hydrated phosphate compounds formation. The decrease in intensities of the peaks at 1020 cm^{-1} and 1080 cm^{-1} is due to the superposition of the P-O-P stretching vibrations between 900 to 1200 cm^{-1}.

The comparison of thermograms of Chrysophosphate® and chrysotile fibers indicates an increase of weight loss between 30 to 250°C for phosphated fibers, and a sharply reduced weight loss of brucite associated with the crysotile fibers, which decomposition appears in the zone between 250 and 400°C. The major dehydroxylation peak (DTG) between 500 and 780°C is modified for the treated samples. The thermograms also indicate a slight change in the rate of dehydroxylation of chrysotile. These observations indicate that $POCl_3$ initially reacts with alkaline impurities ($Mg(OH)_2$, $MgCO_3$ and $CaCO_3$) associated with the chrysotile fibers, forming hydrated magnesium phosphate. The slower rate of dehydroxylation indicates the adsorption or adhesion of magnesium phosphate coming from the impurities reacting with $POCl_3$, and the formation of a phosphate layer involving one or more Mg-O-P bands on the surface. The lower specific surface area of the phosphated fibers (4 compared to 13 $m^2.g^{-1}$) can be attributed to a coating of magnesium phosphate salts on the surface ; it could confirm the encapsulation of the fibers and explain the lesser tendency to adsorb organic compounds.

Figure 2 shows characteristic X-ray emission spectra and electron micrographs of the chrysotile and Chrysophosphate® fibers obtained at 25 keV electron bombardment in the backscattered electron detection mode. Beside the three major elemental constituents (magnesium, silicon and iron), a small contribution of chlorine and calcium, can be observed in the X-ray spectrum. In addition, phosphorus and chlorine become detectable in the Chrysophosphate®. Also it can be noted that the texture of the $POCl_3$-treated fibers is maintained.

Table 1 shows concentrations of a few elements present at the outer surface layers of the chrysotile and Chrysophosphate® fibers, as measured with XPS. Whereas, in the case of Chrysophosphate®, a slight decrease in concentration can be observed for Mg, Si and O, compared to chrysotile, a significant contribution of P (4.4 %) and Cl (3.1 %) has to be noted which can be related to the presence of phosphate groups as reaction products at the outer fiber surface.

Table 1. Concentration of a few elements present at the outer surface layers of chrysotile and Chrysophosphate®, as measured with XPS.

element	concentration (%) chrysotile	Chrysophosphate®
Mg	25.4	18.2
O	43.0	39.6
Si	19.2	13.4
P	-	4.4
Cl	-	3.1

Results of the analysis of the chrysotile and Chrysophosphate® sample are given in Table 2.

Table 2. Chemical composition of standard chrysotile and Chrysophosphate® samples, as measured with ED-XRF.

Element	Standard samples (wt %) chrysotile	Chrysophosphate®
K	0.065 ± 0.0080	0.102 ± 0.012
Ca	0.128 ± 0.035	0.490 ± 0.055
Ti	0.016 ± 0.004	0.019 ± 0.006
Ba	0.033 ± 0.007	0.032 ± 0.006
V	0.009 ± 0.002	0.012 ± 0.003
Cr	0.140 ± 0.011	0.109 ± 0.008
Mn	0.127 ± 0.010	0.103 ± 0.008
Fe	5.60 ± 0.40	4.78 ± 0.35
Co	0.061 ± 0.006	0.045 ± 0.005
Ni	0.152 ± 0.012	0.118 ± 0.009
Cu	< 0.0022	< 0.0022
Zn	< 0.0022	< 0.0025
Ga	< 0.0011	< 0.0012
Ge	< 0.0015	< 0.0016
As	< 0.0015	< 0.0016
Br	0.0014± 0.0004	< 0.0012
Rb	< 0.0010	< 0.0011
Sr	< 0.0013	< 0.0014
Y	< 0.0019	< 0.0020
Hg	< 0.0023	< 0.0025
Pb	< 0.0024	< 0.0025
Mg	19.00 ± 1.50	17.50 ± 1.50
Al	0.82 ± 0.08	1.08 ± 0.10
Si	20.10 ± 1.50	22.50 ± 1.70
S	0.049 ± 0.012	0.043 ± 0.015
Cl	0.28 ± 0.03	2.07 ± 0.16
P	0.14 ± 0.03	2.24 ± 0.18

They were obtained from energy-dispersive X-ray emission spectrometry, according to a procedure

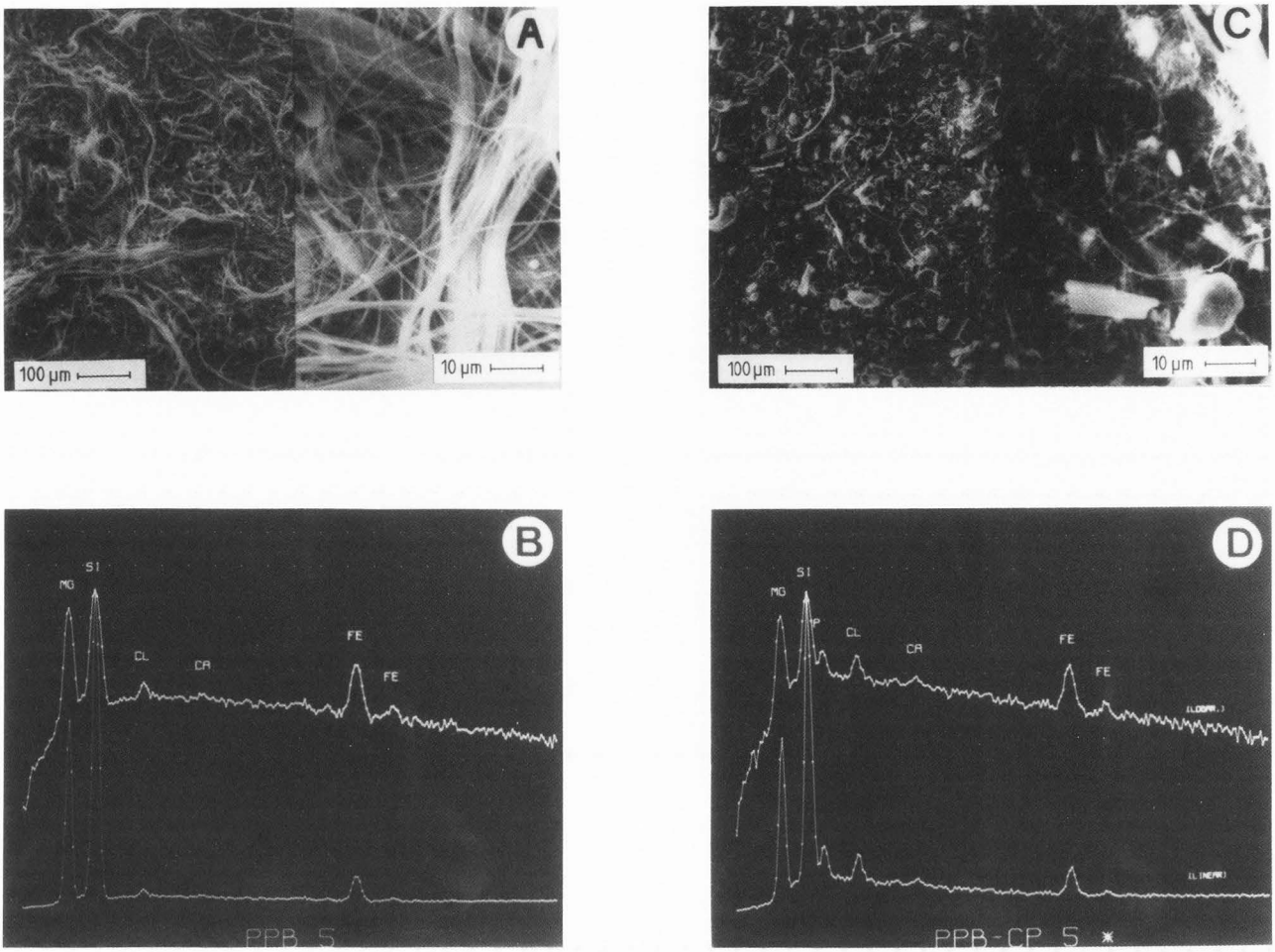

Fig. 2. Characteristic X-ray spectra and electron micrographs of standard chrysotile (left) and Chrysophosphate® (right) fibers, obtained at 25 keV electron bombardment in the backscattered electron detection mode.

published elsewhere (Van Espen, 1978). Besides the three major elemental constituents (magnesium, silicon and iron), a small contribution of calcium, chromium, manganese, nickel and aluminium can be observed for both samples, indicating the variation of ionic substitution into the fiber crystal structure (mainly bivalent cations). For Chrysophosphate® a significant increase in phosphorus and chlorine concentration because of the $POCl_3$-treatment is apparent.

Laser microprobe mass analysis

To characterize the surface structure of the chrysotile and Chrysophosphate® fibers, LAMMA-measurements were performed in laser desorption conditions. The study required the elaboration of a computer analysis of the recorded mass spectra (De Waele, 1985), allowing for the summation of up to 20 spectra in order to be able to gather reproducible information on the reaction behaviour of $POCl_3$ towards chrysotile fibers.

Figures 3 and 4 show the average positive mass spectra of 20 individual analyses of chrysotile and Chrysophosphate® obtained at three laser energies with average laser irradiance of 0.1 µJ, 0.4 µJ and 0.7 µJ. For both standards a representation of the standard deviation on channel intensity is also shown, showing that most of the significant features have a reproducibility of 20-30 %.

The positive mass spectra of the raw chrysotile fibers are characterized by a number of elemental mass peaks from the isotopes of the major constituents in the material : Mg, Si, Fe with some less intense ion peaks of Al, Ti, Cr and Mn. Noteworthy is that in the spectra taken at the lowest laser energy, besides Mg-peaks, which are the only high intensity features in the average spectrum, only a small Fe-ion peak is observed. This is in accordance with results published by Jolicoeur et al. (1981), Stroink et al. (1980) and Sharrock (1982) ; surface iron is normally attributed to the presence of magnetite

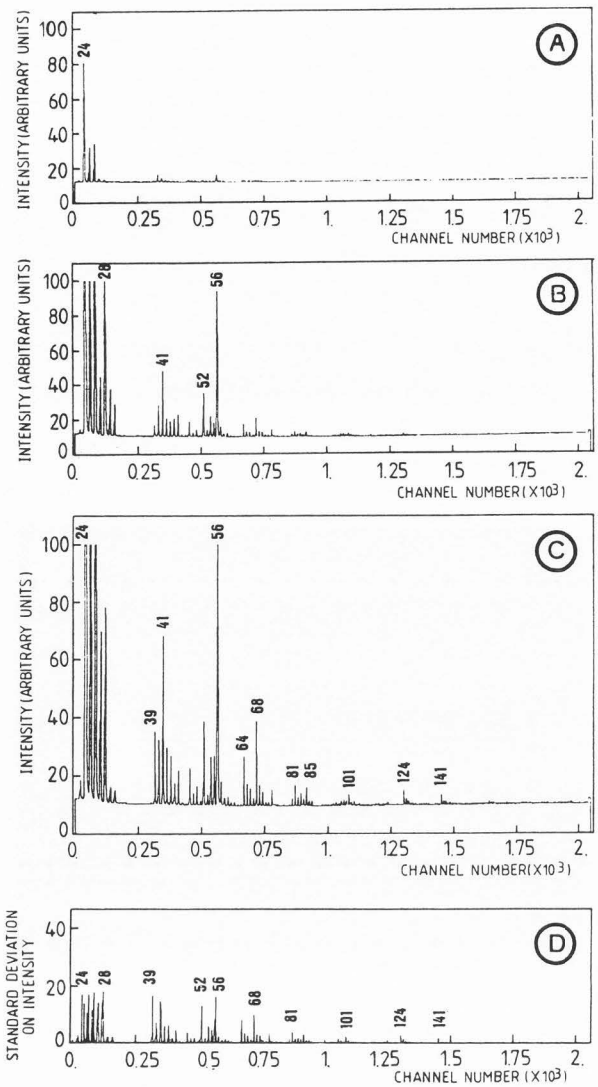

Fig. 3. Average positive mass spectra of 20 individual analyses of chrysotile standard fibers, obtained at three laser energies with average laser irradiance of 0.1 μJ (A), 0.4 μJ (B), and 0.7 μJ (C), with a representation of the standard deviation (D) for the spectrum at 0.7 μJ.

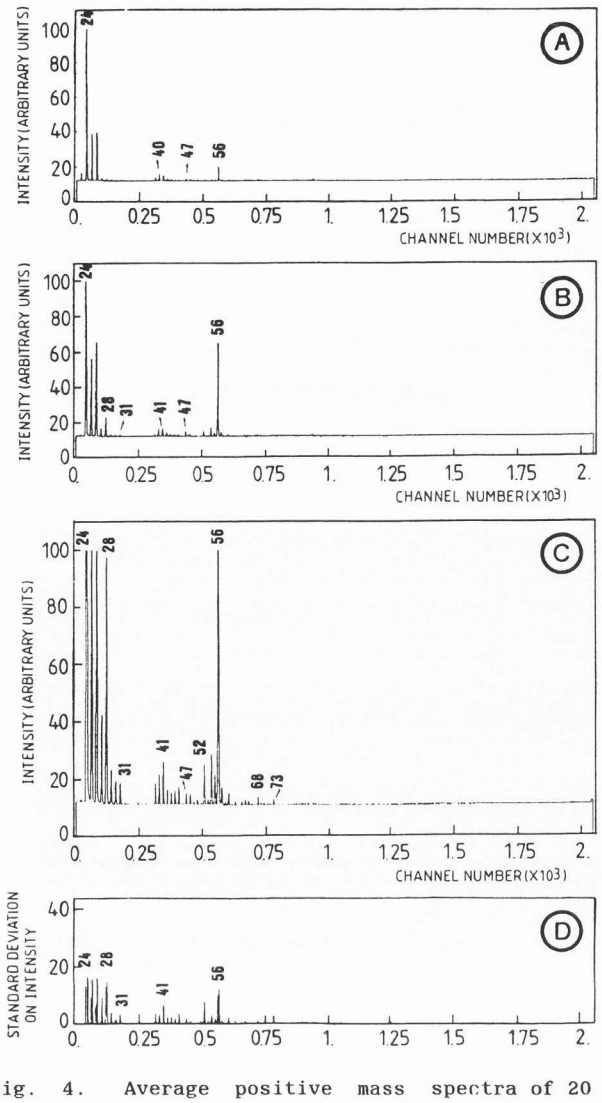

Fig. 4. Average positive mass spectra of 20 individual analyses of chrysotile and Chrysophosphate® standard fibers, obtained at three laser energies with average laser irradiance of 0.1 μJ (A), 0.4 μJ (B), and 0.7 μJ (C), with a representation of the standard deviation (D) for the spectrum at 0.7 μJ.

as a separate phase on the surface of Canadian chrysotile fibers. At higher laser energies, the chrysotile spectra are characterized by a fragmentation pattern of the brucite outer layer and the magnesium silicate layer with characteristic peaks at m/e = 40 (MgO), 41 (MgOH), 56 (MgO_2 ; Fe) and in a few cases also 68 (MgSiO), 81 (Mg_2O_2H) and 85 ($MgSiO_2H$). For the positive mass spectra of a Chrysophosphate® fiber (Figure 4), in the lowest laser energy range, no significant differences in mass spectrum can be observed, compared with an untreated chrysotile fiber. At higher energies, beside the detection of the phosphorus peaks at m/e = 31 (P) and 47 (PO), a significant reduction of the peak intensity at m/e = 41 is observed, indicating the presence of phosphate groups and the removal of the outer brucite layers, respectively.

The negative spectra of chrysotile and Chrysophosphate® fibers provide other interesting information. Figures 5 and 6 represent cumulative negative mass spectra of 20 individual analyses of chrysotile and Chrysophosphate®, obtained at two laser energy ranges with average laser irradiance of 0.3 μJ and 0.6 μJ. In Figures 5C and 6C, for both fiber standards, the standard deviation of a spectrum is represented. Again it can be noted that most of the significant features have a reproducibility of 20-30 %.

The negative spectra for both standards are characterized by the magnesium silicate cluster ions from the chrysotile unit cell : m/e = 60 (SiO_2), 76 (SiO_3), 77 ($HSiO_3$), 100 ($MgSiO_3$) and

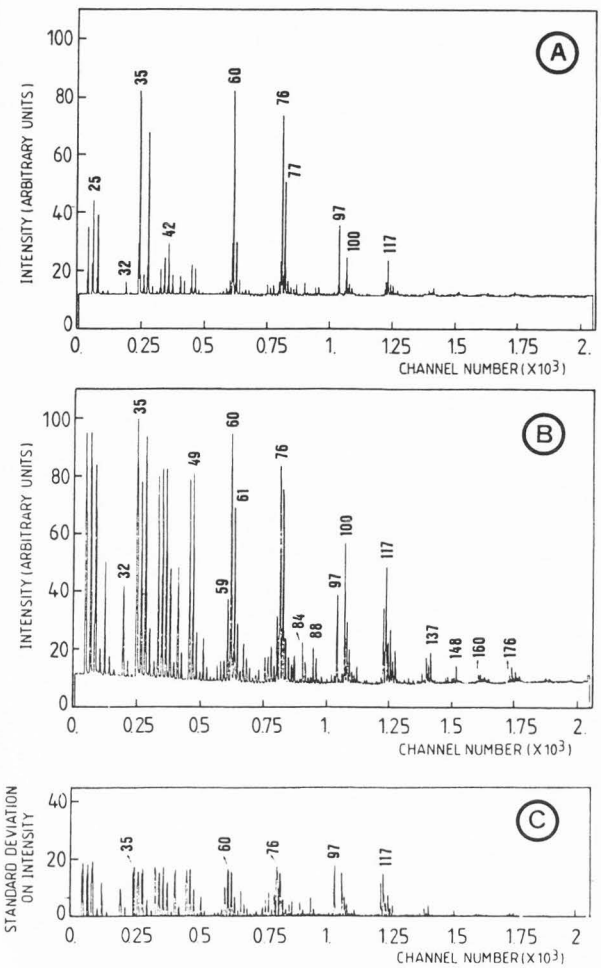

Fig. 5. Average negative mass spectra of 20 individual analyses of chrysotile standard fibers, obtained at two laser energies with average laser irradiance of 0.3 μJ (A), and 0.6 μJ (B), with a representation of the standard deviation (C) for the spectrum at 0.6 μJ.

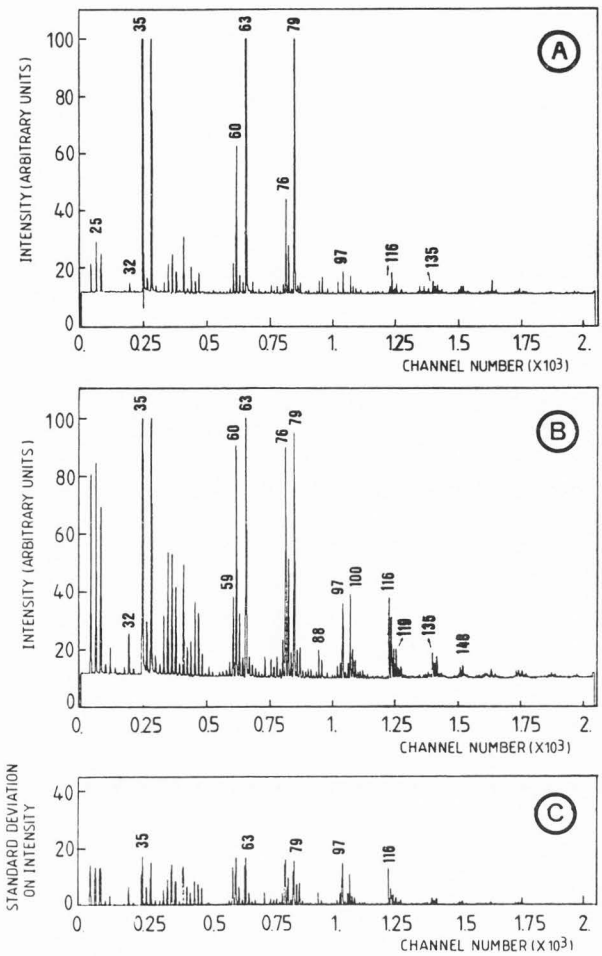

Fig. 6. Average negative mass spectra of 20 individual analyses of Chrysophosphate® standard fibers, obtained at two laser energies with average laser irradiance of 0.3 μJ (A) and 0.6 μJ (B), with a representation of the standard deviation (C) for the spectrum at 0.6 μJ.

117 ($MgOHSiO_3$). The spectra of Chrysophosphate® show in both laser energy ranges intense peaks at m/e = 35 (Cl), 63 (PO_2) and 79 (PO_3), which clearly indicate the existence of phosphate groups in the Chrysophosphate® fiber structure.

By studying the typical fragmentation pattern of the Chrysophosphate® fiber, additional information can be gained on the nature of gaseous $POCl_3$ towards the original chrysotile fibers, through the 2 possible reaction pathways shown in Figure 1. Reaction can occur either on the hydroxyl groups of the outer brucite layer (pathway 1) or on the outer silanol groups (pathway 2). A detailed study of the typical cluster ions in the negative mass spectra rather favors the formation of product B through pathway 1 because most of these ions can be attributed to fragments of phosphate groups adhered to the magnesium silicate skeleton of the fibrils : m/e = 100 ($MgSiO_3$), 116 ($MgSiO_4$), 117 ($MgSiO_3(OH)$), 119 ($MgO_2(PO_2)$) and 135 ($MgO_2(PO_3)$). This hypothesis, which assumes the preservation of the original fibril structure, is even more pronounced by the detection of an intense magnesium elemental peak in the cumulative positive mass spectra of Chrysophosphate®.

The reproducibility of the measurement of positive and negative mass spectra is in general excellent, as follows from the data in Tables 3 and 4, where spectra of chrysotile and Chrysophosphate® are given. Both tables summarize average absolute intensities and standard deviations for 20 individual measurements at the three (positive spectra, Table 3) and two (negative spectra,Table 4) above mentioned laser energies. In accordance with the statements made in previous paragraphs, again the preservation of the original magnesium silicate structure in Chrysophosphate® can be observed through the detection of intense magnesium and silicon elemental peaks in the positive spectra and Mg/Si/O containing cluster ions in the negative spectra. The appearance of the phosphorus peaks at m/e = 31 and 47 (positive spectra) and at m/e = 63, 79, 119, 135, 163 and 179 (negative

Table 3. Average absolute intensities and standard deviations of elemental and cluster positive ion peaks, for 20 individual measurements on chrysotile and Chrysophosphate® standard fibers, and an average laser irradiance of 0.1, 0.4 and 0.7 μJ.

positive ions		chrysotile standard			Chrysophosphate® standard		
m/e	assignment	0.1μJ	0.4μJ	0.7μJ	0.1μJ	0.4μJ	0.7μJ
23	Na	n.d.	22±7	60±30	19±14	n.d.	n.d.
24	Mg	680±300	2060±220	2320±210	750±100	1080±190	1930±1500
27	Al	15±8	250±90	570±200	6±3	39±18	260±70
28	Si	7±3	1250±270	910±210	2±2	110±50	950±190
31	P	n.d.	n.d.	n.d.	n.d.	7±3	73±30
39	K	n.d.	49±25	150±110	15±9	9±4	56±25
40	MgO	20±13	130±50	190±60	26±11	34±14	87±30
41	MgOH	13±8	230±100	450±140	21±6	41±20	93±45
48	Mg_2	11±5	57±20	100±30	n.d.	9±4	27±9
52	Cr	n.d.	220±100	250±90	n.d.	22±14	110±60
55	Mn	n.d.	73±20	140±30	n.d.	15±10	92±18
56	Fe	37±17	1050±180	1320±180	55±16	440±150	1320±140
64	Mg_2O	n.d.	37±18	110±50	n.d.	n.d.	10±5
68	MgSiO	n.d.	67±30	180±70	n.d.	n.d.	18±5
73	FeOH	n.d.	27±11	36±14	n.d.	n.d.	11±7
81	Mg_2O_2H	n.d.	16±8	40±20	n.d.	n.d.	n.d.
85	$MgSiO_2H$	n.d.	14±7	38±20	n.d.	n.d.	n.d.

n.d. = not detected

Table 4. Average absolute intensities and standard deviations of elemental and cluster negative ion peaks, for 20 individual measurements on chrysotile and Chrysophosphate® standard fibers, at an average laser irradiance of 0.3 and 0.6 μJ.

negative ions		chrysotile standard		Chrysophosphate® standard	
m/e	assignment	0.3μJ	0.6μJ	0.3μJ	0.6μJ
32	S	29±9	300±110	18±5	130±50
35	Cl	700±280	1240±170	960±90	1340±130
43	AlO	41±18	330±130	29±7	260±90
59	AlO_2	30±10	300±100	25±6	270±160
60	SiO_2	590±230	1100±240	200±40	800±180
61	SiO(OH)	120±40	580±170	31±7	200±50
63	PO_2	6±2	40±12	840±170	1110±110
76	SiO_3	470±180	910±260	120±25	790±170
77	$SiO_2(OH)$	280±100	670±200	58±10	360±90
79	PO_3	7±3	58±20	590±130	808±150
84	$MgSiO_2$	21±12	120±40	4±3	23±6
88	FeO_2	11±7	86±30	24±9	70±20
97	HSO_4 ; H_2PO_4	180±100	330±140	31±13	280±160
100	$MgSiO_3$	95±40	440±140	12±4	250±70
116	$MgSiO_4$	42±20	200±70	5±3	190±70
117	$Mg(OH)SiO_3$	85±40	330±110	8±4	180±40
119	$MgO_2(PO_2)$	n.d.	n.d.	15±5	82±21
135	$MgO_2(PO_3)$	n.d.	n.d.	15±5	88±23
136	FeO_5	5±3	61±12	n.d.	36±7
137	$Fe(OH)O_4$	16±7	80±20	n.d.	56±20
148	$FeSiO_4$	n.d.	15±7	n.d.	28±6
156	Mg_2SiO_5	n.d.	n.d.	n.d.	7±3
160	$MgSi_2O_5$	n.d.	35±10	n.d.	15±5
163	$MgSiO_3(PO_2)$	n.d.	n.d.	8±3	26±8
176	$MgSi_2O_6$	n.d.	24±7	n.d.	21±6
179	$MgSiO_3(PO_3)$	n.d.	n.d.	6±3	18±6

n.d. = not detected

spectra) and the significant reduction of the $[MgOH]^+$ ion intensity at m/e = 41 for Chrysophosphate® clearly demonstrate that reaction with gaseous $POCl_3$ has taken place at the surface of the original chrysotile fibrils.

Study of chrysotile and Chrysophosphate® leaching

Many data have already been provided by experiments carried out *in vitro* (Harington et al., 1971 ; Davies et al., 1974 ; Wade et al., 1976) and *in vivo* (Wagner et al., 1973 ; Holmes and Morgan, 1967 ; Morgan and Holmes, 1985) in which the biological and carcinogenic activity of chrysotile was compared with that of other asbestos varieties. It was established that chrysotile is highly unstable in acidic solution because structural magnesium is rapidly dissolved from the fiber structure (Chowdhury, 1973, 1975). Leaching of magnesium has been observed after treatment not only with hydrochloric acid (Morgan et al., 1971) but also with various organic acids from the Krebs cycle, the most efficient of which was found to be oxalic acid (Thomassin et al., 1976 ; Goni et al., 1979). Magnesium may also be lost *in vivo*, as observed in fibers isolated from human lungs and from rabbit alveolar macrophages in culture (Langer et al., 1972). It was also found that unleached and leached chrysotile fibers differ in their biological activities *in vitro* (haemolysis, albumin adsorption, enzyme release by macrophages) (Beck et al., 1971; Jaurand et al., 1977). It appeared therefore that size is not the only factor involved in the induction of pleural cancers by mineral fibers. Other parameters that may play a role in the biological activities of inorganic particles are crystallinity (Langer et al., 1978 ; Zitting and Skytta, 1979), surface charge (Light and Wei, 1977a, 1977b) and physico-chemical properties (Beck et al., 1971 ; Morgan et al., 1977). Prolonged acid treatment severely modified one or several of these parameters and in that way interferes with the carcinogenic effect of fibrous dusts. Thus, certain physico-chemical changes occurring intracellularly might have the same effects as acid-treatment and modify the pathogenicity of inhaled fibers in the lung. According to Becklake (1983) the complexity of these mechanisms requires that further investigations are necessary.

In this section, results of a semi-quantitative and qualitative leaching study of chrysotile and Chrysophosphate® fibers in oxalic acid and succinate salt buffer solutions with EPXMA and LAMMA are presented, which demonstrate clearly the potential of these sensitive surface analytical tools for the analysis of natural, physico-chemically modified and depleted fibers. Also we report the verification of these results with those obtained by AAS for the measurement of the leached magnesium and iron concentration in solution.

Dissolution kinetics of chrysotile in oxalic acid studies by XPS and SIMS

A systematic study on the dissolution kinetics of chrysotile in 0.050 M oxalic acid was made earlier by Thomassin et al. (1977) using XPS where the variation of the surface composition was studied as a function of reaction time and temperature. According to these authors, proton transfer and Mg^{2+} complexation might be ruled out as the rate determining steps, involved in the reaction of the chrysotile mineral with the oxalic acid solution, because they are much too fast. Further, it could be assumed that diffusion of Mg^{2+} from the reaction site to the solution through the fibrous silicagel, is rate determining since a plot of the logarithm of the diffusion coefficient versus the reciprocal temperature results in a straight line. As the transport of magnesium from the surface to the bulk of the solution is faster than the transport to the surface in the material, the transport within the sample is the limiting step in the total dissolution process.

A similar study was made by Verlinden et al. (1984) and Swenters et al. (1985) using secondary ion mass spectrometry. In-depth analysis in untreated chrysotile fibers did not show a significant depletion or enrichment of magnesium or silicon at the surface with respect to the bulk. Typical in-depth profiles obtained after treatment by oxalic acid showed that individual layers of fibers with an average thickness of ca. 15 nm are clearly detectable. After treatment, magnesium was always depleted at the surface, whereas the secondary ion signal of silicon remained nearly constant. This observation was in agreement with the analytical results obtained by Thomassin et al. (1977) : after 24 h attack by 0.050 M oxalic acid, no silicon was detected in the solution using a sensitive AAS-method. Also, according to Johan et al. (1974), the texture of the fiber is maintained even if the major part of the magnesium is extracted.

Quantitative analysis

Results of a systematic study using AAS on the magnesium and iron leaching of chrysotile and Chrysophosphate® in 0.050 M oxalic acid (non-stirred medium at 20°C) with treatment times between 5 min and 208 h are presented in Figure 7, where the sum of the Mg and Fe concentration is plotted versus the square root of the treatment time.

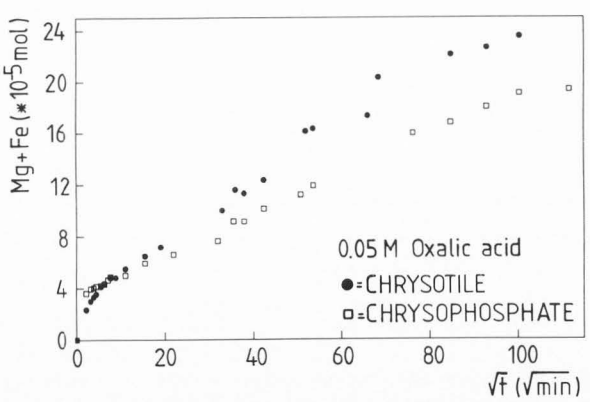

Fig. 7. Sum of the magnesium and iron concentration in leaching solutions of chrysotile and Chrysophosphate® fibers in 0.050 M oxalic acid (non-stirred solution, 20°C), versus the square root of the treatment time.

Earlier it was found that the relative fractional release of magnesium (F) from chrysotile in similar experiments (obtained by complexometric titration) as a function of the treatment time corresponds to the relationship $F = a + b.\sqrt{t}$ (Swenters et al., 1985).

From the results obtained here, it is obvious that the Mg and Fe leaching for both chrysotile and Chrysophosphate® becomes more important with increasing treatment time. However, it can be noted that below a treatment time of ca. 100 min, a higher amount of Mg and Fe seems to be leached from Chrysophosphate®. This may be due to the fact that water adsorbed onto the original chrysotile standard fibers may hydrolyze $POCl_3$ to phosphoric acid with production of HCl, during the gaseous industrial treatment. In this way, besides silanol groups at the chrysotile outer surface layers, also $MgCl_2$ and reaction water can be formed as byproducts, which may contaminate the Chrysophosphate® fibers produced. Also iron, present as a magnetite impurity at the chrysotile fiber surface, can react in the same way. Hence, during the first moments of Chrysophosphate® treatment with 0.050 M oxalic acid, the $MgCl_2$ will be dissolved more quickly in comparison to the outer brucite ($Mg(OH)_2$) layers at the surface of chrysotile fibers. At longer treatment periods, less Mg and Fe is leached from the Chrysophosphate® fibers because magnesium phosphate is less soluble than magnesium hydroxide.

Some characteristic X-ray emission spectra and electron micrographs of chrysotile and Chrysophosphate® fibers, subjected to a 0.050 M oxalic acid treatment during 30 min, 30 h and 168 h, are shown in Figure 8. In general, it can be noted that, even after 168 h, the texture of the treated fibers is maintained and that the Mg/Si intensity ratio for both standards decreases with increasing treatment periods. Also, it appears that a small contribution of phosphorus remains detectable in the Chrysophosphate® spectrum even after a long leaching time.

More detailed microstructural fiber information before and after leaching is obtained using the electron microscope at high magnification. Figures 9A and B show detailed EM pictures of standard Chrysophosphate® fibrils, obtained at 80 keV electron bombardment. The lighter parts on the fibrils can be ascribed to residual traces of $MgCl_2$ after $POCl_3$-treatment. After 168 h oxalic acid leaching (Figure 9D) these traces seem to be removed from the fibril surface, in comparison to original and treated (Figure 9C) chrysotile fibrils which remain visually unchanged after leaching.

In order to study the influence of the oxalic acid concentration on the chrysotile and Chrysophosphate® dissolution rate, leaching experiments were performed using 0.050 M, 0.100 M and 0.666 M oxalic acid at ambient temperature. The measured concentrations of Mg and/or Fe in the leaching solution are summarized in Tables 5 and 6. From the results it is obvious that for both standards, the Mg and Fe leaching becomes more important as the molarity increases. Again, after longer treatment periods, more pronounced leaching is observed from chrysotile compared to Chrysophosphate® fibers. Similar conclusions can be drawn from dissolution experiments with 0.050 M oxalic acid at different temperatures, with results presented in Table 6. In this table also long-time leaching of succinate salt buffer experiments at 37°C are included showing clearly the lesser Mg and Fe dissolution characteristics of both fiber standards in simulated in vivo conditions. Again it has to be noted that enhanced leaching for Chrysophosphate® in such environment can possibly be explained by the better dissolution of surface-adhered $MgCl_2$ in comparison to $Mg(OH)_2$ at the chrysotile fiber surface.

Table 5 : Magnesium and iron concentration in the leaching solution of chrysotile and Chrysophosphate® fibers in 0.100 M oxalic acid (non-stirred medium at 20°C), as measured with AAS.

Sample	treatment time (min)	measured concentration values ($x10^{-5}$mol) magnesium	iron
chrysotile	15	4.07±0.05	0.28±0.05
	30	4.17±0.05	0.30±0.02
	60	4.81±0.05	0.49±0.02
	120	5.72±0.05	0.56±0.02
	240	6.74±0.05	0.86±0.02
	480	8.72±0.05	1.12±0.02
	1440	13.32±0.05	1.47±0.05
	1500	13.86±0.05	1.33±0.05
	2880	17.9 ±0.2	1.70±0.02
	5760	21.2 ±0.3	1.89±0.02
	10080	25.41±0.05	1.19±0.05
Chrysophosphate®	15	4.28±0.05	0.30±0.02
	30	4.44±0.05	0.28±0.02
	60	4.44±0.05	0.28±0.02
	120	4.81±0.05	0.28±0.05
	240	5.72±0.05	0.33±0.02
	480	6.63±0.05	0.49±0.02
	1440	10.00±0.05	0.62±0.05
	1500	10.16±0.05	0.72±0.02
	2880	12.63±0.05	0.82±0.02
	5760	17.9 ±0.4	1.40±0.02

Laser microprobe mass analysis : To verify whether LAMMA in laser desorption conditions provides a way for probing small changes in inorganic fiber surface composition a study was made on the leaching of magnesium and other elements of interest at the surface and interior regions of chrysotile and Chrysophosphate® fibers in oxalic acid and succinate salt buffer solution.

First, the positive mass spectra of the treated standard fiber samples were studied in order to check possible intensity differences of magnesium elemental and cluster ion peaks due to leaching phenomena during several leaching periods at different reaction temperatures.

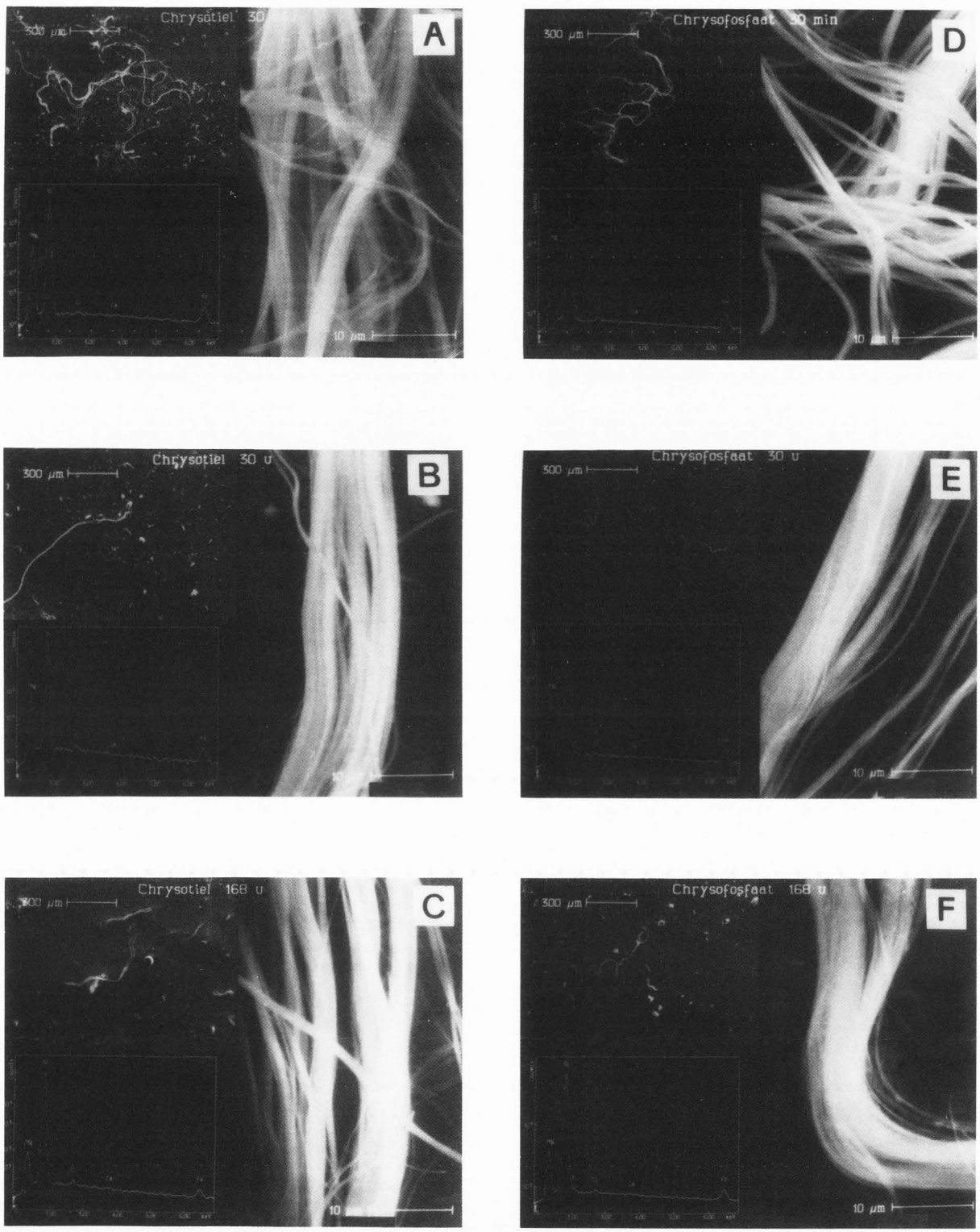

Fig. 8. Characteristic X-ray spectra and electron micrographs of chrysotile (left) and Chrysophosphate® (right) fibers subjected to 0.050 M oxalic acid treatment during 30 min (A,D), 30 h (B,E) and 168 h (C,F), obtained at 25 keV bombardment in the backscattered electron detection mode.

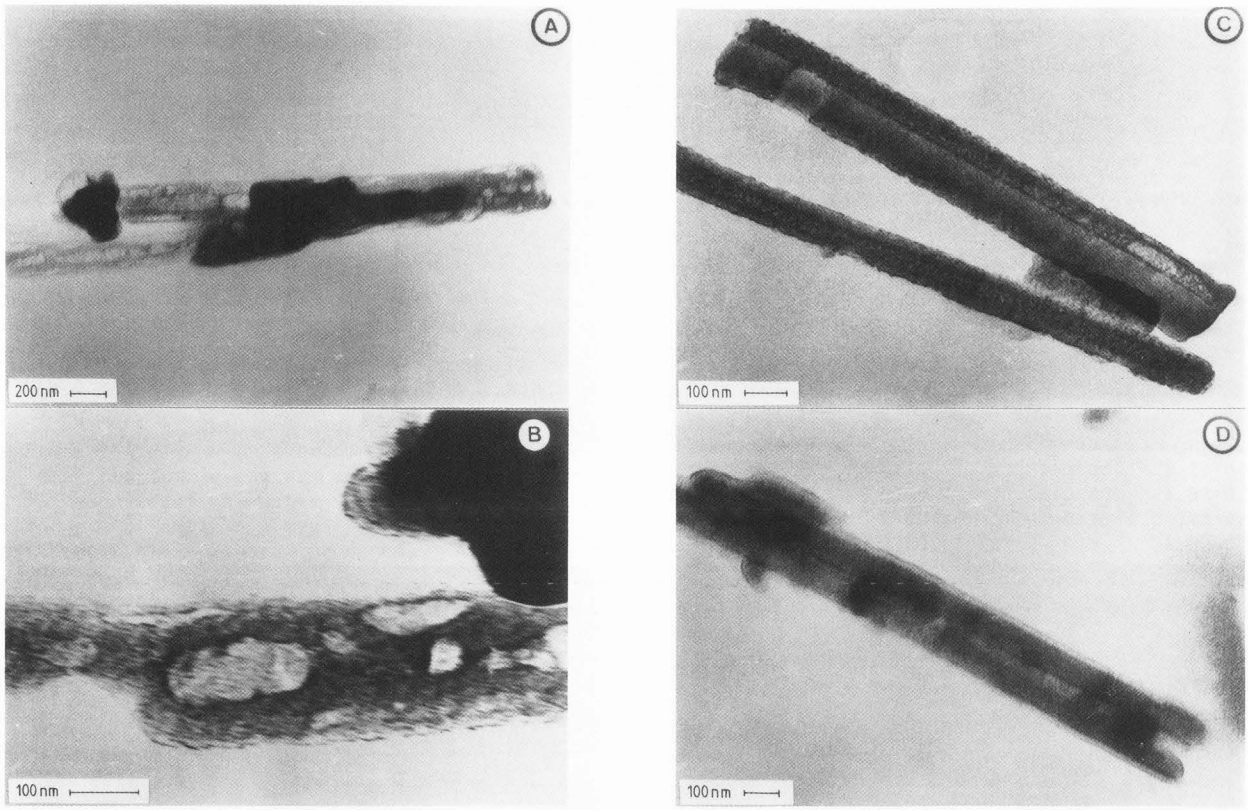

Fig. 9. Typical detailed electron microscope pictures of standard Chrysophosphate© fibrils (A and B), and of chrysotile (C) and Chrysophosphate© (D) fibrils after 0.050 M oxalic acid treatment during 168 h. The internal fibril diameter is ca. 10 nm, the external diameter ca. 25 nm.

Table 7 summarizes average relative intensities to ^{28}Si = 100 and standard deviations of elemental and cluster positive ions, for 20 individual measurements on chrysotile and Chrysophosphate® fibers, subjected to different oxalic acid and succinate salt buffer treatments, at an average laser irradiance of 0.7 μJ. At the treated chrysotile and Chrysophosphate® fiber surface, the intensity ratio of the Mg^+ (m/e = 24), MgO^+ (40), $MgOH^+$ (41), Fe^+ (56), Mg_2O^+ (64) and $Mg_2O_2H^+$ (81) ion peaks relative to Si^+ (m/e = 28) decreases significantly with increasing leaching time and treatment temperature, compared with untreated standard fibers. These intensity ratios seem to be somewhat higher in non-stirred solution as compared to the stirred one. This is in accordance with SIMS-results obtained by Verlinden et al. (1984) which suggest that convection forces may enhance diffusion to some extent, so that the surface Mg-composition is higher in non-stirred experimental conditions. After long treatment periods (168 h) or at high temperature (80°C), the ion intensity ratios become minimum, due to the brucite and/or magnesium phosphate depletion from the fibril structure and the continuous acid diffusion into the chrysotile and Chrysophosphate®. Because of the production of silanol groups at the fiber surface, a slight increase in ($SiOH^+/Si^+$) intensity ratio can also be observed.

Table 8 summarizes average relative intensities to $(SiO_2)^-$ = 100 (m/e = 60) and standard deviations of elemental and cluster negative ions, obtained at an average laser irradiance of 0.6 μJ, for 20 individual measurements on the oxalic acid and succinate salt buffer treated fiber standards. Compared with untreated chrysotile and Chrysophosphate®, the intensity ratio of the $[SiO(OH)]^-$ (m/e = 61), $[SiO_2(OH)]^-$ (77), $[MgSiO_3]^-$ (100), $[MgSiO_2(OH)]^-$ (101), $[MgSiO_4]^-$ (116) and $[MgSiO_3(OH)]^-$ (117) ion peaks relative to $[SiO_2]^-$ (m/e = 60) decreases significantly with increasing leaching time (stirred and non-stirred solution), probably due to the partial destruction of the magnesium-silica skeleton by continuous diffusion of oxalic acid into the fiber structure and to migration of the silica and -Mg-O-Si-O- units from the interior region towards the depleted fiber surface. Moreover, for Chrysophosphate® it can be noted that the $[PO_2]^-/[SiO_2]^-$ and $[PO_3]^-/[SiO_2]^-$ intensity ratio gradually decreases with increasing leaching time and treatment temperature, because of the possible breakdown of the phosphate groups, present at the Chrysophosphate® fibril surfaces. Figure 10 gives characteristic examples of average negative mass spectra (20 individual analyses) of

Table 6. Magnesium and iron concentration in the leaching solutions of chrysotile and Chrysophosphate® fibers, during 1440 min at different temperatures in 0.050 M, 0.100 M and 0.666 M oxalic acid and in succinate salt buffer, as measured with AAS.

experimental leaching data		measured concentration values ($x10^{-5}$ mol)			
medium	temperature (°C)	magnesium		iron	
		chrysotile	Chrysophosphate®	chrysotile	Chrysophosphate®
0.050M oxalic acid	20	10.33±0.05	8.35±0.03	0.979±0.004	0.783±0.005
0.100M oxalic acid	20	13.32±0.05	10.00±0.05	1.47 ±0.05	0.62 ±0.05
0.666M oxalic acid	20	19.3 ±0.3	13.6 ±0.3	1.37 ±0.02	0.51 ±0.02
0.050M oxalic acid	50	24.98±0.05	22.7 ±0.2	1.49 ±0.02	0.84 ±0.05
0.050M oxalic acid	80(*)	23.97±0.05	24.9 ±0.2	0.95 ±0.02	1.56 ±0.05
Succinate salt buffer	37	0.68 ±0.01	2.29±0.01	0.02 ±0.01	0.03 ± 0.01

(*) 420 min treatment time instead of 1440 min.

Table 7. Average relative intensities to ^{28}Si = 100 and standard deviations of elemental and cluster positive ion peaks, for 20 individual measurements on chrysotile (C) and Chrysophosphate®(CP) fibers subjected to different oxalic acid and succinate salt buffer treatments, at an average laser irradiance of 0.7 μJ.

Positive ions		sample	standard	0.05 M oxalic acid						succinate salt buffer
				room temperature			1 h treatment		1 h stirring	
m/e	assignment			30 min	30 h	168 h	50°C	80°C	at room temperature	888 h 37°C
24	Mg	C	420±80	290±120	180±40	150±26	160±50	150±40	200±50	240±50
		CP	640±310	250±80	170±60	140±30	200±60	180±45	220±70	190±65
40	MgO	C	60±30	52±35	7±3	4.4±1.6	5±3	8±2	8±3	1.7±0.7
		CP	160±80	16±7	12±7	5±2	13±6	5±2	6±3	5±2
41	MgOH	C	76±45	70±45	4.4±1.8	2.9±0.9	4±3	11±4	3.0±0.9	3.5±1.3
		CP	120±60	21±10	13±7	4.4±1.9	13±7	8±3	16±10	6±3
45	SiOH	C	3.3±1.9	2.4±1.6	1.6±0.8	10±5	n.d.	8±3	1.1±0.5	1.5±0.6
		CP	7±4	5±2	8±4	9±3	2.8±1.3	3.0±1.2	2.5±1.5	1.2±0.5
56	Fe	C	130±60	100±60	52±16	51±14	40±20	30±9	46±16	16±5
		CP	270±130	70±30	42±18	34±11	55±20	33±12	51±20	46±25
64	Mg_2O	C	50±30	8±5	0.9±0.3	1.4±0.5	n.d.	0.5±0.3	n.d.	n.d.
		CP	88±45	2.2±0.9	0.5±0.3	0.6±0.2	1.9±0.6	0.8±0.4	3.7±1.9	1.3±0.7
81	Mg_2O_2H	C	26±15	13±7	n.d.	2.1±0.8	n.d.	n.d.	n.d.	n.d.
		CP	19±10	1.9±0.9	n.d.	n.d.	n.d.	1.5±0.6	0.8±0.4	n.d.

n.d. = not detected

Table 8. Average relative intensities to $[SiO_2]^-$ = 100 (m/e = 60) and standard deviations of elemental and cluster negative ion peaks, for 20 individual measurements on chrysotile (C) and Chrysophosphate® (CP) fibers, subjected to different oxalic acid and succinate salt buffer treatments, at an average laser irradiance of 0.6 μJ.

Negative ions		sample	standard	0.05 M oxalic acid						succinate salt buffer
				room temperature			1 h treatment		1 h stirring	
m/e	assign-ment			30 min	30 h	168 h	50°C	80°C	at room temperature	888 h 37°C
35	Cl	C	72±25	17±6	47±12	17±6	32±16	5±2	61±26	44±21
		CP	87±55	46±14	13±4	36±15	52±11	28±12	38±17	105±20
61	SiO(OH)	C	22±8	36±11	36±10	52±17	23±8	23±7	34±10	40±13
		CP	12±8	31±10	40±8	36±15	23±5	35±14	28±9	17±4
76	SiO_3	C	100±30	104±25	99±23	102±29	110±40	115±20	110±30	100±30
		CP	100±70	97±20	110±23	90±30	90±13	90±40	130±40	77±14
77	$SiO_2(OH)$	C	58±19	61±17	70±23	88±26	71±25	69±14	75±22	90±25
		CP	29±18	59±20	86±19	74±35	57±17	71±29	74±28	56±11
100	$MgSiO_3$	C	28±9	43±13	39±10	51±17	47±19	34±9	61±20	22±8
		CP	28±17	48±16	69±11	40±17	30±9	23±10	78±28	19±15
101	$MgSiO_2(OH)$	C	8±3	15±6	11±4	21±7	14±5	7.6±1.9	21±7	8±3
		CP	3.3±1.9	15±4	25±5	9±4	8±2	5±2	32±14	4.4±1.2
116	$MgSiO_4$	C	15±6	37±11	25±7	36±12	32±16	22±6	33±11	11±3
		CP	20±11	26±7	49±10	19±10	15±5	16±5	61±26	3.5±0.9
117	$MgSiO_3(OH)$	C	26±9	36±11	26±7	55±17	38±17	26±8	48±19	27±10
		CP	6±3	44±18	73±10	41±19	24±7	16±6	68±30	18±4
63	PO_2	CP	129±85	66±20	77±11	61±30	83±17	30±13	78±30	180±30
79	PO_3	CP	110±70	35±13	59±10	51±24	47±15	31±13	68±27	171±25

chrysotile and Chrysophosphate® fibers, subjected to a 1 h treatment with 0.050 M oxalic acid, at room temperature (stirred solution) and at 50°C and 80°C (non-stirred solution), obtained at an average laser irradiance of 0.6 μJ.

As confirmed earlier with SIMS (Verlinden et al., 1984), complexometric titration (Swenters et al., 1985) and XPS (Thomassin et al., 1977) these leaching phenomena can be explained by considering the crystal structure of chrysotile asbestos fibers. Chrysotile has a layered structure, with magnesium atoms between two siloxane layers (-Si-O-) and the sheets rolled. Acid leaching of chrysotile leaves a pseudomorph of silica which retains the original -Si-O-Si- network as shown by Atkinson and Rickards (1971). When oxalic acid passes through the layered sheets, it first washes out magnesium hydroxide (brucite) leaving the skeleton of -Si-O- units which, being small and fragile, break way. These units remain in a colloidal state since they can be hydrolyzed to orthosilicic acid (Hodgson, 1979). In the continuous leaching of chrysotile with increasing treatment times, there is an initial high release of Mg^{2+}, which subsequently reduces to a steady rate after several days. Correspondingly, there is an initial minimal release of silica, increasing to a much higher steady rate, probably in the form of fragmentary -Si-O- (Chowdhury, 1973, 1975).

From the above results one can conclude that LAMMA may provide a powerful though qualitative tool for probing small changes in inorganic surface composition. The decreased intensity of the elemental and molecular constituents at the treated fiber surface as measured with LAMMA in laser desorption conditions can be compared with those obtained by real depth-profiling with SIMS. In general, the apparent changes in composition measured by LAMMA are much more pronounced than those measured with SIMS. Therefore, LAMMA depth-profiling only yields semi-quantitative information, but cannot be relied on in a quantitative manner (De Waele, 1985).

Adsorption and reaction behaviour towards organic adsorbents

It has been reported earlier that there exists a synergetic effect of a number of organic

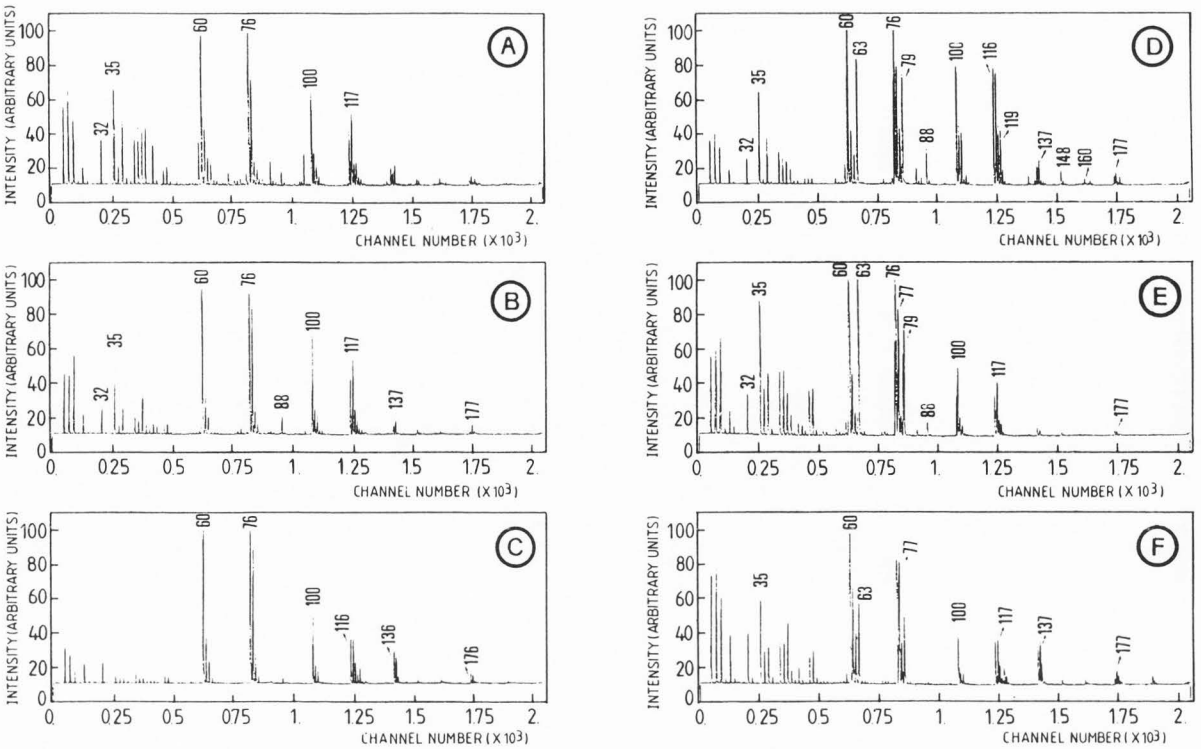

Fig. 10. Average negative mass spectra of 20 individual analyses of chrysotile (left) and Chrysophosphate® (right) fibers, subjected to a 1 h 0.050 M oxalic acid treatment at room temperature (A,D) (stirred solution) and at 50°C (B,E) and 80°C (C,F) (non-stirred solution). All spectra were obtained at an average laser irradiance of 0.6 μJ.

pollutants when they are associated with asbestos pollution (Harington et al., 1975).

In this respect, compounds in tobacco smoke appear to be one of the more active (Selikoff et al., 1968, 1980 ; Liddell, 1981). The hypothesis that the toxicity of asbestos is correlated with the adsorption power of carcinogenic organic pollutants or precursors of carcinogenic compounds (Contour et al., 1978, 1980), can only be studied with sensitive surface analytical methods. The potential of LAMMA for the characterization of the asbestos fiber surface appeared from the authors work which attempted the detection of accidental surface contaminants (De Waele et al., 1983c) and also of organic impurities adsorbed onto the asbestos surface using several adsorption processes (De Waele and Adams, 1985, 1986).

In order to study the differences in adsorption behaviour and reaction capability between natural and chemically modified chrysotile, LAMMA-analysis was performed on chrysotile and Chrysophosphate® fibers treated with benzo[a]pyrene (BaP), N,N-dimethylaniline (DMA) and ortho-phenylenediamine (OPDA). The methodology of these measurements is described in detail elsewhere (De Waele et al., 1983a, 1983b, 1984a).

Benzo[a]pyrene : Many reports indicate that the carcinogenic (genotoxic) potential of BaP may be enhanced several fold by the promoter effect of asbestos fibers (Reiss et al., 1983 ; Mossman and Craighead, 1981). Using high performance liquid chromatography (HPLC), it has been observed that BaP has a great affinity for natural asbestos fibers (Ménard et al., 1984), and that chemical modification of natural chrysotile with $POCl_3$ results in a reduction of specific surface area (4 instead of 13 $m^2.g^{-1}$) and a significant loss of this adsorption potential of the compound (Ménard et al., 1986).

In order to check the adsorption behaviour of natural and modified chrysotile, we subjected both samples to an identical treatment with 10^{-3} M BaP in benzene solution. Table 9 summarizes the average results for at least 15 measurements for two successive laser energy (E_1) ranges : $E_1 < 0.4$ μJ (average : 0.25 μJ) and $E_1 > 0.4$ μJ (average : 0.65 μJ). The BaP molecular ion peak at m/e = 252 (M_{BaP}) can be detected at much higher intensity in the spectra of chrysotile compared with those of Crysophosphate®. For the lowest and highest energy range, a reduction of ca. 50 % and 70 %, respectively, of adsorption potential can be observed for Chrysophosphate® compared to chrysotile.

N,N-dimethylaniline and ortho-phenylene-diamine : The oxidative properties of clay minerals and fibrous particles have been studied with DMA and OPDA, which adsorb and then react at the fiber surface yielding coloured products. The oxidation products of DMA (Vansant and Yariv,

Table 9. Intensities of important cluster ion peaks for chrysotile and Chrysophosphate® fibers treated with benzo[a]pyrene (BaP), N,N-dimethyl-aniline (DMA) and ortho-phenylenediamine (OPDA), taken at two different laser energy (E_l) ranges.

	m/e	chrysotile		Chrysophosphate®	
		E_l<0.4μJ	E_l>0.4μJ	E_l<0.4μJ	E_l>0.4μJ
BaP	252	11.3±1.6	19.3±1.9	5.7±0.7	6.2±0.8
DMA	120	38±6	162±12	16±4	22±4
	134	4.0±0.5	13±4	3.4±0.6	4.8±0.5
	253	2.4±0.4	5.0±1.0	1.6±0.3	2.5±0.6
	358	1.5±0.4	2.6±0.4	1.5±0.3	1.5±0.3
	372	1.7±0.5	1.0±0.3	0.5±0.2	0.5±0.3
OPDA	184	9.2±1.6	21±4	3.5±0.5	8±2
	211	54±6	117±19	19±3	29±6

1977) and OPDA (Sidgwick, 1966 ; Finar, 1973) formed, appeared to depend on the structural characteristics of the mineral. Both surface properties and the presence of active sites are important.

The detection of DMA and OPDA oxidation products on asbestos fibers with LAMMA has provided interesting information on the surface adsorption capacity and reactivity (De Waele and Adams, 1985, 1986). It therefore allows single procedures for the evaluation of the hazard of industrially produced fibrous dusts, such as Chrysophosphate®.

In order to check whether the DMA-oxidation reaction sequence also occurs with chemically modified chrysotile, the adsorption of DMA onto pure chrysotile and Chrysophosphate® was studied. Therefore, the intensity of typical ion peaks around m/e = 120, 134, 253, 358 and 372, which correspond with the several DMA oxidation products (De Waele et al., 1983b), was measured. These ion peaks occur at somewhat higher intensity in the positive mass spectra of the treated chrysotile as compared with those of treated Chrysophosphate®. Semi-quantitative results (at least 15 measurements) are presented in Table 9 which summarizes the intensity differences of these typical organic ions for the same laser energy ranges as mentioned in previous paragraphs. In general, the affinity of DMA and its oxidative behaviour towards Chrysophosphate® fibers results in a loss of about 60 and 85 % of adsorption potentials (m/e = 120) for the lowest and highest energy range, respectively.

In order to control whether the OPDA oxidation scheme also occurs with Chrysophosphate®, the adsorption of OPDA onto pure and phosphated chrysotile was studied. As observed previously with DMA, again a decrease in adsorption and reaction behaviour can be concluded for the Chrysophosphate® fibers. Table 9 again summarizes intensity differences of the characteristic ion peaks at m/e = 184 and 211, which correspond with the major OPDA oxidation products (De Waele et al., 1984a). In general, a loss of about 65 and 75 % of adsorption and reaction potential can be observed for Chrysophosphate®, for the lowest and highest energy range, respectively.

In general, from these three different adsorption species, it can be concluded that, in contrast with untreated chrysotile, the $POCl_3$ treatment of chrysotile fibers seems to result in a reduced but not complete lost potential of the resulting Chrysophosphate® fibers to adsorb polycyclic hydrocarbons and some organic reference probes. An average loss of adsorption potential of (58 ± 7) % and even (76 ± 9) % can be observed for measurements at the low and higher laser energy range, all measured in the same experimental and instrumental operating conditions. This reduced adsorption potential is, in all probability, related to the adhesion of magnesium phosphate on the outer fibril layers. These semi-quantitative LAMMA results are in accordance with those obtained by Ménard et al. (1986) who studied the adsorption potential on bulk samples using HPLC.

Conclusions

LAMMA, supplemented with other sensitive analytical methods was used to obtain a detailed knowledge of the chrysotile and Chrysophosphate® surface properties, such as surface micro-structure, elemental composition and chemical functionality, nature and reactivity of surface defects and catalytic sites, etc. The examples shown illustrate semi-quantitatively that laser mass spectrometry, used in laser desorption conditions, provides valuable information on the chemical composition of the natural and modified fiber surface. Attention was given to the surface modification in chrysotile and Chrysophosphate® on chemical attack by oxalic acid and succinate salt buffer treatment. Organic compounds when adsorbed on the surface, were used for the determination of the adsorption capacity and the reactivity of the fiber surface. In correlation with biomedical investigations, this study could contribute to the elucidation of the potential sequences of fiber surface properties in relation to the biological activity and cytotoxicity.

Acknowledgement

This research was funded by the E.E.C. through research grant no. ENV-620-B(RS). JKDW is indebted to the National Fund for Scientific Research (N.F.W.O., Belgium), for financial support. The authors gratefully acknowledge substantial help by several members of the U.I.A. Chemistry department, namely, H. Nullens, W. Van Mol, L. Leysen, W. Van Borm, K. Vinck and P. Veny.

References

Atkinson AW, Rickards AL. (1971). Physics and Chemistry of asbestos Minerals. 2nd Int. Conf., Louvain, September 6-9, 1971, paper 3.1.

Beck EG, Holt PF, Nasrallah ET. (1971). Effects of Chrysotile and Acid-treated Chrysotile on Macrophages Cultures. Brit. J. Ind. Med. 28, 179-185.

Becklake MR. (1983). Occupational Lung Disease - Past Record and Future Trend using the Asbestos Case as an example. Clin. & Investig. Med. 6, 305-317.

Chisholm JE. (1983). Transmission Electron Microscopy of Asbestos. Asbestos Volume 2 : Properties, Applications and Hazards, Chissick SS and Derricott R (eds), John Wiley & Sons, Chichester, 85-167.

Chowdhury S. (1973). Surface Chemical Studies of Asbestos Minerals. Ph.D. Thesis, Dept. Mining & Mineral Techn., Univ. London, UK.

Chowdhury S. (1975). Kinetics of Leaching of Asbestos Minerals at Body Temperature. J. Appl. Chem. Biotechnol. 25, 347-353.

Chrysotile Asbestos Test Manual (1974). Asbestos Textile Institute Inc. and Quebec Asbestos Mining Association, 3rd edn. (Revised 1978), Canada.

Contour JP, Guèrin I, Mouvier G. (1978). A Study of the Adsorption of Organic Micro-pollutants on Chrysotile and Crocidolite. Atmosph. Pollut. 1, 255.

Contour JP, Guèrin I, Mouvier G. (1980). Adsorption de Polluants Organiques Amines sur des Fibres d'Amiante. Environm. Pollut. (Sèries B) 1, 234.

Cook JD, Smith ET. (1979). Dealing with Asbestos Problems. Asbestos Volume 1 : Properties, Applications and Hazards, Michaels L, Chissick SS (eds), John Wiley & Sons, Chichester, 279-304.

Cossette M. (1983). De l'Amiante moins toxique grace à la Phosphorylation. GEOS 1, 16-18.

Davies P, Allison AC, Ackerman J, Butterfield A, Williams S. (1974). Asbestos Induces Selective Release of Lysosomal Enzymes from Mononuclear Phagocytes. Nature 251, 423-425.

Denoyer E, Van Grieken RE, Adams FC, Natusch DF. (1982). Laser Microprobe Mass Spectrometry. 1 : Basic Principles and Performance Characteristics. Anal. Chem. 54, 26A-32A.

Derricott R. (1979). The Use of Asbestos and Asbestos-Free Substitutes in Buildings. Asbestos Volume 1, Properties, Applications and Hazards, Michaels L, Chissick SS (eds), John Wiley & Sons, Chichester, 305-338.

De Waele JK, Vansant EF, Van Espen P, Adams FC. (1983a). Laser Microprobe Mass Analysis of Asbestos Fiber Surfaces for Organic Compounds. Anal. Chem. 55, 671-677.

De Waele JK, Vansant EF, Adams FC. (1983b). Laser Microprobe Mass Analysis of N,N-dimethylaniline and Catalytic Oxidation Products on the Fiber Surface of Asbestos Standards. Mikrochim. Acta II(5-6), 367-384.

De Waele JK, Gybels JJ, Vansant EF, Adams FC. (1983c). Laser Microprobe Mass Analysis of Plastic Contaminated Asbestos Fiber Surfaces. Anal. Chem. 55, 2255-2260.

De Waele JK, Vansant EF, Adams FC. (1984a). Laser Microprobe Mass Analysis (LAMMA) of Ortho-phenylenediamine on Asbestos Fibers. Anal. Chim. Acta 161, 37-51.

De Waele JK, Luys MJ, Vansant EF, Adams FC. (1984b). Analysis of chrysotile Asbestos by LAMMA and Mössbauer Spectroscopy; a Study of the Distribution of Iron. J. Trace & Microprobe Techn. 2(2), 87-103.

De Waele JK. (1985). Characterization of Asbestos Fiber Surfaces by Laser Microprobe Mass Analysis (LAMMA). Ph.D. Thesis, U.I.A. University of Antwerp, Dept. Chemistry.

De Waele JK, Adams FC. (1985). Applications of LAMMA for characterization of Asbestos. Scanning Electron Microsc. 1985; III : 935-946.

De Waele JK, Adams FC. (1986). Laser Microprobe Mass Analysis of Fibrous Dusts Chapter 16. In : Physical and Chemical Characterization of Individual Airborne Particles. Spurny K R. (ed.). Ellis Horwood Ltd., Chichester, 271-297.

Doll R, Peto J. (1985). Asbestos; Effects on Health of Exposure to Asbestos. Her Majesty's Stationary Office, Health & Safety Commission H.M.S.O., London.

Dunnigan J, Nadeau D, Paradis D, Pele JP, Calvert R, Lalancette JM, Cossette M. (1980). Cytotoxic and Haemolytic Effect of Natural and Chemically Modified Chrysotile. Proc. 4th Int. Conf. Asbestos, Torino, May 26-30, 1980, 747-772.

Finar IL. (1973). Organic Chemistry, Vol. 1, The fundamental Principles, Longman Gray Ltd., London, 6th Edn., p. 66.

Fletcher RA, Chabay I, Weitz DA, Chung JC. (1984). Laser Desorption Mass Spectrometry of Surface-Adsorbed Molecules. Chem. Phys. Letters 104, 615-619.

Gadsden IA, Parker I, Smith WL. (1970). Determination of Chrysotile in Airborne Asbestos by an IR Spectrometric Technique. Atmosph. Envir. 4, 667-670.

Goni J, Thomassin JM, Jaurand MC, Touray JC. (1979). Photoelectron Spectroscopy Analysis of Asbestos Dissolution in Acidic media of Biological Interest. Origin and distribution of the Elements, LH. Ahrens (ed.), Pergamon Press, Oxford, 807-817.

Gorski CH, Stettler LE. (1974). The Surface Energetics of Asbestos Minerals. Amer. Ind. Hyg. Assoc. J. June, 345-353.

Harington JC, Allison AC, Badami DV. (1975). Mineral Fibers : Chemical, Physico-chemical and Biological Properties. Adv. Pharmacol. Chemother. 12, 291-402.

Harington JS, Miller K, McNab G. (1971). Haemolysis by Asbestos. Environm. Res. 4, 95-117.

Hodgson AA. (1979). Chemistry and Physics of Asbestos. Asbestos Volume 1, Properties, Applications and Hazards, Michaels L, Chissick SS (eds), John Wiley & Sons, Chichester, 67-114.

Holmes A, Morgan A. (1967). Leaching of Constituents of chrysotile Asbestos in vivo. Nature 215, 441.

Hronovsky V, Plaisner U, Benda R. (1975). A Modified Plaque Method for Arboviruses on Plastic Funnels. Acta Virol. 19, 150.

Jaurand MC, Sèbastien P, Bignon J, Goni J. (1977). Leaching of Chrysotile Asbestos in Human Lungs. Correlation with in vitro studies using Rabbit Alveolar Macrophages. Environm. Res. 14, 245-254.

Johan Z, Goni I, Sarcia C, Bonnaud G, Bignon J. (1974). Influence de certains Acides Organiques sur la Stabilité du Chrysotile. Adv. Organic Geochemistry. 1973, Paris, Technip, 893-903.

Jolicoeur C, Roberge P, Fortier JL. (1981). Separation of Short Fibers from Bulk Chrysotile Asbestos Fiber Materials : Analysis and Physico-Chemical Characterization. Can. J. Chem. 59, 1140-1148.

Kimmerle FM, Khorami J, Choquette D. (1982). Thermal Analysis of Phosphated Chrysotile Fibers. Proc. 7th Int. Conf. Thermal Analysis, Ontario, Miller B (ed), John Wiley & Sons, Chichester, 614-619.

Lalancette JM, Dunnigan J. (1981). Novel Phosphated Asbestos Fibers. US-Patent no. 4.356.057.

Langer AM, Rubin IB, Selikoff IJ, Pooley FD. (1972). Chemical Characterization of Uncoated Asbestos Fibers from the Lungs of Asbestos Workers by Electron Microprobe Analysis. J. Histochem. Cytochem. 20, 735-740.

Langer AM, Wolff MS, Rohl AN, Selikoff IJ. (1978). Variation of Properties of Chrysotile Asbestos Subjected to Milling. J. Toxicol. Environm. Health 4, 173-188.

Liddell FD.(1981). Biological Effects of Mineral Fibers. Wagner JC (ed), IARC Scientific Publ. no. 30, vol. 2, Lyon, 661.

Light WG, Wei ET. (1977a). Surface Charge and Haemolytic Activity of Asbestos. Environm. Res. 13, 135-145.

Light WG, Wei ET. (1977b). Surface Charge and Asbestos Toxicity. Nature 265, 537-539.

Luys MJ, De Roy G, Vansant EF, Adams FC. (1982). Characteristics of Asbestos Minerals : Structural Aspects and Infra-red Spectra. J. Chem. Soc., Faraday Trans. 1, 78, 3561-3571.

Macnab G, Harington JS. (1967). Haemolytic Activity of Asbestos and Other Mineral Dusts. Nature 214, 522-533.

McDonald JC. (1985). Health Implications of Environmental Exposure to Asbestos. Environm. Health Persp. 62, 319-328.

Mènard H, Noël L, Khorami J, Jouve JL, Dunnigan J. (1986). The Adsorption of Polyaromatic Hydrocarbons on Natural and Chemically-Modified Asbestos Fibers. Environm. Res. 40, 84-91.

Mènard H, Noël L, Kimmerle FM, Tousignant L, Lambert M. (1984). Adsorption Isotherms of Polycyclic Aromatic Hydrocarbons on Asbestos Chrysotile by High-Pressure Liquid Chromatography. Anal. Chem. 56, 1240-1242.

Morgan A, Holmes A. (1985). The Enigmatic Asbestos Body : its Formation and Significance in Asbestos-Related Disease. Environm. Res. 38, 283-292.

Morgan A, Holmes A, Gold G. (1971). Studies of the Solubility of Constituents of Chrysotile Asbestos in vivo using Radioactive Tracer Techniques. Environm. Res. 4, 558-570.

Morgan A, Davies P, Wagner JC, Berry G, Holmes A. (1977). The Biological Effects of Magnesium-leached Chrysotile Asbestos. Brit. J. Exp. Pathol. 58, 465-473.

Mossman BT, Craighead JE. (1981). Mechanisms of Asbestos Carcinogenesis. Environm. Res. 25, 269-280.

Nauman AW, Dresher WH. (1966). The Morphology of Chrysotile Asbestos as inferred from Nitrogen Adsorption Data. The Amer. Mineralogist 51, 711-725.

Pezzoli PA. (1979a). Asbestos Treatment with Metal Molybdates. US-Patent no. 4.171.405, October 16, 1979.

Pezzoli PA. (1979b). Asbestos Treatment with Metal Tungstates. US-Patent no. 4.168.346, September 18, 1979.

Reiss B, Tong C, Telang S, Williams GM. (1983). Enhancement of Benzo[a]pyrene Mutagenicity by Chrysotile Asbestos in Rat Liver Epithelial Cells. Environm. Res. 31, 100-104.

Schnitzer RJ, Pundsack FL. (1970). Asbestos Haemolysis. Environm. Res. 3, 1-13.

Selikoff IJ, Hammond EC, Churg J. (1968). Asbestos Exposures, Smoking and Neoplasia. J. Amer. Med. Assoc. 204, 106-112.

Selikoff IJ, Seidman H, Hammond EC.(1980). Mortality Effects of Cigarette Smoking among Amosite Asbestos Factory Workers. J. Natl. Cancer Inst. 65, 507-513.

Sharrock P. (1982). Chrysotile Asbestos Fibers from Quebec : Electron Magnetic Resonance Identification. Geochim. & Cosmochim. Acta 46, 1311-1315.

Sidgwick N. (1966). Aromatic Amines. The Organic Chemistry of Nitrogen, Chapter 5. Oxford Press, 3rd Edn., Miller and Springall, p. 182.

Société Nationale de l'Amiante (1981). Novel Phosphated Asbestos Fibers. Great-Britain Patent no. 2076383, December 2, 1981.

Stroink G, Blaauw C, White CG, Leiper W. (1980). Mössbauer Characteristics of UICC Standard Reference Samples. Can. Mineralogist 18, 285-290.

Swenters IM, De Waele JK, Verlinden JA, Adams FC. (1985). Comparison of SIMS and Complexometric Titration for the Determination of Leaching of Magnesium from Chrysotile Asbestos. Anal. Chim. Acta 173, 377-380.

Tabet JC, Cotter RJ. (1983). Time-Resolved Laser Desorption Mass Spectrometry II. Measurement of the Energy Spread of Laser Desorbed Ions. Int. J. Mass Spectrom. & Ion Phys. 54, 151-158.

Thomassin JH, Goni J, Baillif P, Touray JC. (1976). Etude par Spectrométrie ESCA des Premiers Stades de la Lixiviation du Chrysotile en Milieu Acide Organique. C.R. Acad Sci. Paris 283 Série D, 131-134.

Thomassin JH, Goni J, Baillif P, Touray JC, Jaurand MC. (1977). An XPS Study of the Dissolution Kinetics of Chrysotile in 0.1 N Oxalic Acid at different temperatures. Phys. Chem. Minerals 1, 385-398.

Van der Peyl GJ. (1984). Desorption and Ionization Processes in Laser Mass Spectrometry. Ph. D. Thesis, University of Amsterdam.

Van Espen P. (1978). Fotonengeïnduceerde Röntgenfluorescentie-analyse van Aërosolen. Ph.D. Thesis, U.I.A., University of Antwerp, Dept. Chemistry, 1978.

Vansant EF, Yariv S. (1977). Adsorption and Oxidation of N,N-Dimethylaniline by Laponite. J.

Chem. Society, Faraday Trans I, 73, 1815-1824.

Verbueken AH, Bruynseels FJ, Van Grieken RE. (1985). Laser Microprobe Mass Analysis : a Review of Applications in the Life Sciences. Biomed. Mass Spectrom. 12, 438-463.

Verlinden JA, De Waele JK, Swenters IM, Adams FC. (1984). Secondary Ion Mass Spectrometric Analysis of Leaching of Magnesium from Chrysotile in Oxalic Acid Solution. Surf. Interface Anal. 6, 286-290.

Vogt H, Heinen MJ, Meier S, Wechsung R. (1981). LAMMA®-500 Principle and Technical Description of the Instrument. Fresenius Z. Anal. Chem. 308, 195-200.

Wade MJ, Lipkin LE, Tucker RW, Frank AL. (1976). Asbestos Cytotoxicity in a long-term Macrophage-like cell Culture. Nature 264, 444-446.

Wagner JC, Berry G, Timbrell V. (1973). Mesothelioma in Rats after Inoculation with Asbestos and Other Materials. Brit. J. Cancer 28, 173-185.

Whittacker EJ. (1953). The Structure of Chrysotile. Acta Cryst. 6, 747-748.

Whittacker EJ. (1955). The Diffraction of X-Rays by a Cylindrical Lattice. Acta Cryst. 8, 261-271, 726-729.

Whittacker EJ. (1956). The Structure of Chrysotile. Acta Cryst. 8, 855-867.

Yada K. (1971). Study of Microstructure of Chrysotile Asbestos by High Resolution Electron Microscopy. Acta Cryst. A27, 659-664.

Zitting A, Skytta E. (1979). Biological Activity of Titanium Dioxides. Int. Arch. Occup. Environm. Health 43, 93-97.

Zussman J. (1979). The Mineralogy of Asbestos. Asbestos Volume 1 : Properties, Applications and Hazards, Michaels L, Chissick SS (eds), John Wiley & Sons, Chichester, 45-66.

Discussion with Reviewers

J.L. Abraham : Does the treatment of the chrysotile fibers to convert them to Chrysophosphate® result in any change in the fiber diameter, length, clumping, or surface area measurements ? Is there any information on the diameters and aspect ratios of the fibers before and after treatment ?

Authors : As appeared through SEM observation diameter, length, and in general morphology did not change drastically in the treatment. We refer to Figure 2. The surface area decreased from 13 $m^2.g^{-1}$ to 4 $m^2.g^{-1}$ and also the zeta potential decreased from +18 mV to -36 mV.

J.L. Abraham : In Table 2 an increased calcium concentration is shown. What is the explanation of this ?

Authors : We do not have an explanation for the apparent increase of the concentration for Ca and less prominently for K ; perhaps it is the result of contamination.

J.L. Abraham : If the LAMMA depth-profiling only yields semi-quantitative information, under what conditions would you recommend its use rather than SIMS ?

A. Lodding : Would you briefly summarize the chief properties and assets of the LAMMA-technique, that have made it particularly suited for the study of your asbestos material ? How do the advantages compare with other available analytical techniques ?

Authors : Compared to SIMS, LAMMA is considerably less quantitative and especially reproducible, but the advantage resides in the quick cost-effective analysis and the fact that for non-conducting samples as these, no sample preparation is required. The method is rather to be used as a quick exploratory tool. We refer to a previous paper in the same journal for a detailed answer to these questions (De Waele and Adams, 1985).

J.L. Abraham : Given the most interesting analogy between the process of producing Chrysophosphate® from chrysotile and the process of alteration of asbestos fibers in tissues, in which phosphate and iron are deposited along with other organic materials - rendering the fiberless biologically active - do you have any comments on the similarities and dissimilarities as far as biologic toxicity is concerned ? What types of studies and time frame are projected to determine if the Chrysophosphate® is really safer over a long period of time ? Have there been experimental studies with long fibers to investigate, for example mesothelioma production or fibrosis ?

Authors : Conclusive proof of the long term biological safety of Chrysophosphate® is not yet available to date, but preliminary information indicates significantly less potent cytotoxic properties compared to pure chrysotile. Together with other treatments of the fiber surface such as with EDTA, simple phosphates, disodium versenate, and certain acidic polymers, the deposition of phosphate groups has been found to possess reduced haemolytic activity as evidenced by using red blood cells, and reduced cytotoxicity using the rat pulmonary macrophage test (Dunnigan et al., 1980). Contrary to pure chrysotile, the material has reduced ability to adsorb and carry genotoxic carcinogens, such as benzo[a]pyrene and other polyaromatic hydrocarbons, thus being less likely to contribute to the phenomenon of "synergism", observed in smokers exposed to chrysotile (Ménard et al., 1986).

A. Lodding : How do you take care of the problem of spectral doublets, triplets, etc... in your study, considering the relatively low mass resolution of the LAMMA technique ? How do you know that Si_2 can be neglected ? What about MgSi on mass 52, or AlSi on mass 55, or (Table 4) O_2 on mass 32 ? Finally : are there no appreciable contributions of hydrocarbons and hydrides in your spectra ?

Authors : One of the weaknesses of the method is the low mass resolution of m/e = 700-800. Especially at laser desorption conditions, molecular interferences may be important in the spectra. This is one of the reasons for the

often high inaccuracies obtained with the method. With existing instrumentation it is only possible to attempt to determine the extent of possible interferences from the systematics of the pure spectra. In this work the specific interferences mentioned are not intense enough to be the cause of interferences.